Physics Letters A 383 (2019) 358–365

Contents lists available at ScienceDirect

Physics Letters A

www.elsevier.com/locate/pla

Electric double layer of electrons: Attraction between two like-charged surfaces induced by Fermi–Dirac statistics

Mitja Drab [a,*], Veronika Kralj-Iglič [b]

[a] Faculty of Electrical Engineering, University of Ljubljana, 1000 Ljubljana, Slovenia
[b] Laboratory of Clinical Biophysics, Faculty of Health Sciences, University of Ljubljana, 1000 Ljubljana, Slovenia

ARTICLE INFO

Article history:
Received 16 July 2018
Received in revised form 26 October 2018
Accepted 3 November 2018
Available online 6 November 2018
Communicated by C.R. Doering

Keywords:
Electric double layer
Electrons
Nanocapacitor
Helmholtz free energy
Fermi–Dirac statistics

ABSTRACT

Recently we reported that Fermi–Dirac statistics of electrons contained between two oppositely charged surfaces separated by the order of nanometers create overlapping electric double layers with repulsive total force between the surfaces. Here, we present a new branch of solutions to the same variational problem resulting in higher energy densities and identify regions of the phase space where the force between two like-charged surfaces is attractive.

1. Introduction

Nanomaterials are defined with one of the dimensions being between 1 and 100 nanometers. At and below these scales, classic physical phenomena give way to a variety of quantum effects. Recent years have seen a rapid development of material manipulation at the nanoscale [1–4], ranging from biocompatible materials for use in medicine [5–9] and nanoscale biosensors [10,11] to nanocapacitors [12]. With the advances of nanoengineering, electrochemical capacitors can be made from nanoporous materials that are significantly increasing their energy and power densities [13–17].

The main mechanism of energy storage devices in nanocapacitors is the electric double layer (EDL), a diffuse layer of mobile charges (usually an electrolyte) adsorbed onto an oppositely charged surface [18]. In thermodynamic equilibrium, the electrostatic forces are in balance with the effects of diffusion, resulting in the accumulation of counterions and depletion of like-charged coions at the surface. The first rigorous description of the EDL was derived a century ago by the work of Gouy and Chapman in the form of the Poisson–Boltzmann equation, a first-order mean field approximation of electrostatic and entropy effects. Within the model, the ions of one species were monovalent, point-like and noninteracting, embedded in a continuum of a constant dielectric permittivity [19,20]. Since then, the models of EDL have been improved by including various steric effects like the finite size of ions or their shells of hydration [21–27]. With growing computational power, recent models can simulate the electrolyte molecules directly or include the polar nature of solvents, resulting in an average orientational ordering and a space-dependent dielectric permittivity [28–31].

Experimentally, energy storage at the nanoscale is starting to show promise with nano gap capacitors and vacuum microcathode arrays [32]. It is known that nano vacuum gaps can have higher energy densities than macro scale capacitors because dielectric strength increases as the gap gets smaller [33]. A quick survey of the field reveals that most research is centered around the engineering aspects of electrodes and electrolytes for higher energy and power densities yield, yet quantum effects are likely to be important at the scales of capacitors manufactured at the nanoscale.

Little attention has been given to a quantum treatment of the EDL, with a notable exception that focused on the wave functions of electrons at the electrode interface [34]. The subject of nanosized gaps is however not new and has been investigated in the past in different contexts. Image potentials for tunneling electrons in the gap between two metal surfaces were shown to be relevant in physics of tunneling microscopes [54]. A quantum treatment was recently given to a system of two negatively charged cathodes surrounding a thin, positively charged anode [35]. In this three plate nanocapacitor model, the electron states are quantized even

* Corresponding author.
E-mail address: mitja.drab@fe.uni-lj.si (M. Drab).

https://doi.org/10.1016/j.physleta.2018.11.003
0375-9601/

at room temperatures due to small dimensions. In addition to energy storing technologies, nano gaps separated by ferroelectrics are being considered for use in random access memory applications [33].

In the present paper, we consider a model capacitor with two charged surfaces separated by the order of nanometers. Confined between them are electrons that are quantized because the dimensions are so small. The model is not restricted to electrons, however, but could be extended to other composite fermions with respective mass and charge. Due to asymmetric constraints on the wave functions, their energy levels are governed by Fermi–Dirac statistics that prohibit two particles to occupy the same energy state. Our previous work demonstrated that this quantum constraint results in a diffuse-like distribution of particles between the surfaces in the limits of low temperatures [36]. However, we knowingly focused on only one of the branches of possible solutions. Here, we focus on the omitted solution, relying on a similar functional density theory approach. The difference of both solutions becomes most apparent when we examine the Helmholtz free energy, a thermodynamic potential that is minimal at thermodynamic equilibrium in systems where volume and temperature are held constant [37]. We find portions of the phase space where the free energy has a locally positive gradient, implying a net attractive force between the two like-charged surfaces. This is surprising, although not unheard of in physical systems or molecular models of EDL. Short range attractions between charged mica have been reported on in the presence of divalent ions [38]. Giant unilamellar vesicles with similarly charged phospholipid membranes can attract when oppositely-charged antibodies are present in the solution [39]. The main mechanisms of such attraction are ion-ion correlations and bridging effects due to orientational ordering of ions [39–41]. Molecular dynamics simulations and DFT have confirmed a net attraction in cases where two macroions approach each other, leading to an overlapping of the highly correlated counterion layers [46]. In suspensions containing large and small colloidal particles, the small colloids are excluded from the depletion regions in the vicinity of large colloids, resulting in an osmotic pressure pushing the large colloids together [47,48]. Our model is, in contrast to these investigations, of a purely quantum mechanical origin and takes place orders of magnitude below macroscopic scales.

First, we will briefly present the model and derive the governing equation with references to our previous work, followed by results and a discussion of their significance.

2. The model and the governing equation

Our model system is the same as the one in [36]. Two large planar and parallel surfaces are located at $x = 0$ and $x = d$. Each surface carries a uniformly distributed positive charge with surface charge density $\sigma > 0$. Confined between the surfaces is a single type of negatively charged fermions (electrons), so that the whole system is electrically neutral. A generalization to positively charged particles and negatively charged surfaces is straightforward. The particles are subject to the constraints on available energy states implied in the Fermi–Dirac statistics. These states can be either occupied or unoccupied, with the probability p_n that energy level ε_n is occupied being [37]:

$$p_\mathrm{n} = \frac{1}{1 + \exp\left((\varepsilon_\mathrm{n} - \mu)/k_\mathrm{B}T\right)}, \tag{1}$$

where μ is the Fermi level, k_B is the Boltzmann constant and T is absolute temperature [37]. Note that direct Coulomb interactions between the particles are deliberately omitted due to possible screening of the Fermi–Dirac interaction. For simplicity we take that each particle is confined to an infinite three dimensional square potential well so that its energy is given by quantized discrete values [37]:

$$\varepsilon_\mathrm{n} = \frac{\mathrm{n}^2 h^2}{8ml^2}, \quad \mathrm{n} = 1, 2, 3, \ldots \tag{2}$$

Here, h is the Planck constant, m is the particle mass and l is the extension of the potential well. Following our former derivations [36], the system is divided into thin slices with the width δx parallel to the surfaces so that electric fields are considered constant within the slice. As there are many particles in the system, the energies are assumed to lie close together and the summation in the statistical averages can be replaced by integrals. The average number of particles $\bar{N}$ in each slice of thickness δx is

$$\bar{N} = 2 \cdot (1/8) \int_0^\infty \frac{4\pi n^2}{1 + \exp((\varepsilon_\mathrm{n} - \mu))/k_\mathrm{B}T} \, \mathrm{d}n, \tag{3}$$

with the average energy

$$\bar{E} = 2 \cdot (1/8) \int_0^\infty \frac{4\pi n^2 \varepsilon_\mathrm{n}}{1 + \exp((\varepsilon_\mathrm{n} - \mu))/k_\mathrm{B}T} \, \mathrm{d}n. \tag{4}$$

The factor 2 comes from the two spin states of electrons. In the limit of low temperatures ($T \to 0$), only the lowest energies up to the Fermi level are occupied. In this low temperature limit there is no entropy contribution, since $F = \bar{E} - TS$ [37] and we calculate the Helmholtz free energy of a thin slice due to Fermi–Dirac wave function symmetry constraints on electrons F_sym as [36]:

$$\delta F_\mathrm{sym} = \delta \bar{E} = \frac{3}{5} \left(\frac{h^2}{8m}\right) \left(\frac{3}{\pi}\right)^{2/3} \left(\frac{\bar{N}}{V}\right)^{2/3} \bar{N}. \tag{5}$$

Integrating over the entire gap between the charged surfaces d, we get [36]:

$$F_\mathrm{sym} = \frac{3}{5} \left(\frac{h^2}{8m}\right) \left(\frac{3}{\pi}\right)^{2/3} A \int_0^d n^{5/3}(x) \, \mathrm{d}x, \tag{6}$$

where we introduced a volume density of particles as $n(x) = \bar{N}/A\delta x$ and A is the area of the charged plates (see Fig. 1). Charged particles and surfaces create mean electric fields with electrostatic energy

$$F_\mathrm{el} = \frac{\varepsilon_0 A}{2} \int_0^d E^2(x) \, \mathrm{d}x, \tag{7}$$

where $E(x)$ is the magnitude of the electric field and ε_0 is the permittivity of vacuum. The electric field has only the x component due to planar symmetry. For simplicity we assume that the electric field has no direct influence on the wave functions of electrons, therefore the total free energy is the sum [36]

$$F = F_\mathrm{sym} + F_\mathrm{el}. \tag{8}$$

To obtain a global thermodynamic equilibrium, F is minimized with respect to unknown functions $n(x)$ and $E(x)$. The constraints of the system are the validity of Gauss's law

$$\varepsilon_0 \frac{\partial E}{\partial x} = -e_0 n(x), \tag{9}$$

and electroneutrality

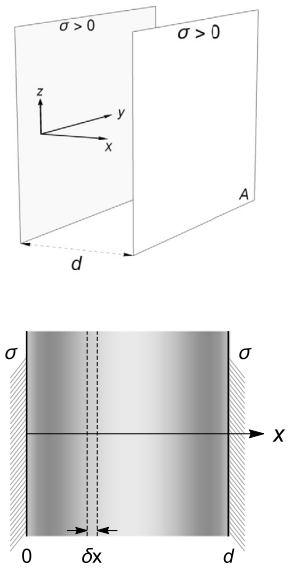

Fig. 1. A schematic of the model with a defined coordinate system. It is presumed that the yz charged surfaces are infinitely large and planar symmetry applies, rendering the problem one-dimensional in x. Here, σ is the surface charge density, d is surface separation and A is the area of the surfaces. The origin of the coordinate system ($x = 0$) is located at the left surface. The gray shading is proportional to particle density $n(x)$ for $k = 5.1$. Note that the maximum particle density is not in the immediate vicinity of the charged surfaces.

$$e_0 \int_0^d n(x)\,\mathrm{d}x = 2\sigma, \tag{10}$$

where e_0 is the elementary charge. For notational convenience, we can rewrite all equations into normalized form

$$x = \tilde{x}/d, \quad n = \tilde{n}/n_0, \quad E = \tilde{E}/E_0, \tag{11}$$

where tilde marks position $\tilde{x}$, number particle density $\tilde{n}$ and electric field $\tilde{E}$ with dimensions. The normalization constants are:

$$n_0 = \frac{2\sigma}{de_0}, \quad \phi_0 = \frac{\sigma d}{\varepsilon_0} \quad \text{and} \quad E_0 = \frac{\sigma}{\varepsilon_0}. \tag{12}$$

The Lagrange function for dimensionless particle density $n(x)$ and dimensionless mean electric field $E(x)$ in the system can now be derived [36]:

$$\mathcal{L} = \alpha n^{5/3}(x) + E^2(x) - \lambda(x)\left(\frac{\partial E(x)}{\partial x} + 2n(x)\right) + \tilde{\lambda} n(x), \tag{13}$$

where $\lambda(x)$ and $\tilde{\lambda}$ are the local and global Lagrangian multipliers ensuring the validity of Gauss's law and constant number of particles within the system, respectively. The dimensionless constant α is equal to [36]:

$$\alpha = \frac{3}{5\sqrt[3]{2}}\left(\frac{3}{\pi}\right)^{2/3} \frac{h^2\varepsilon_0}{me_0^{5/3}} \frac{1}{\sqrt[3]{\sigma d^5}}. \tag{14}$$

Considering the relation $E(x) = -\mathrm{d}\phi/\mathrm{d}x$, the Euler–Lagrange equations give the equation for electric potential $\phi(x)$ in the space between the surfaces (for details, see [36]):

$$\left(\frac{\mathrm{d}^2\phi(x)}{\mathrm{d}x^2}\right)^{2/3} = \left(\frac{\beta\sqrt{5}}{4}\right)^2 (4\phi(x) - \tilde{\lambda}). \tag{15}$$

Here, β is a constant related to α:

$$\beta = 4\sqrt{\frac{2}{5}}\left(\frac{3}{5\alpha}\right)^{3/4}. \tag{16}$$

The symmetry of the system imposes the electric field to be zero between the surfaces [36]:

$$\left.\frac{\mathrm{d}\phi(x)}{\mathrm{d}x}\right|_{x=1/2} = 0, \tag{17}$$

with corresponding constant electric potential

$$\phi(x = 1/2) = 0. \tag{18}$$

The other boundary condition follows from electroneutrality of the system. The electric field at the plates is equal to the surface charge density, which simplifies in normalized units [36]:

$$\left.\frac{\mathrm{d}\phi(x)}{\mathrm{d}x}\right|_{x=0} = -1. \tag{19}$$

In summary, all previous conditions discussed in [36] still apply. We focus on the negative root of equation (15), so we are interested in the case where the right side of (15) is negative,

$$4\phi(x) < \tilde{\lambda}, \tag{20}$$

changing the equation to

$$\frac{\mathrm{d}^2\phi(x)}{\mathrm{d}x^2} = (-1)^{3/2}\left(\frac{\beta\sqrt{5}}{4}\right)^3 (\tilde{\lambda} - 4\phi(x))^{3/2}. \tag{21}$$

3. Results and discussion

Equation (21) was solved for $\phi(x)$ by introducing a new variable and determining the coefficients from boundary conditions as detailed in Appendix A. The final result for the electric potential is:

$$\phi(x) = \frac{1 - \cos\left(k(x - \frac{1}{2})\right)\cosh\left(k(x - \frac{1}{2})\right)}{k\left(\cosh\frac{k}{2}\sin\frac{k}{2} - \cos\frac{k}{2}\sinh\frac{k}{2}\right)}. \tag{22}$$

Here, the constant k is related to β by

$$k = \frac{5^{1/4}}{2}\sqrt{\frac{\beta^3}{2}}. \tag{23}$$

The volume density of charged particles between the surfaces is derived from Euler–Lagrange equations [36]:

$$n(x) = \frac{1}{2}\frac{\mathrm{d}^2\phi(x)}{\mathrm{d}x^2}, \tag{24}$$

which simplifies to

$$n(x) = \frac{k\sin k(x - \frac{1}{2})\sinh k(x - \frac{1}{2})}{\cosh\frac{k}{2}\sin\frac{k}{2} - \cos\frac{k}{2}\sinh\frac{k}{2}}. \tag{25}$$

We immediately see that this function can be less than zero at some values of k, which would imply a negative particle density. We can circumvent this anomaly by investigating the intervals of k where the particle density is non-negative,

$$n(x) \geq 0. \tag{26}$$

The maximum value of k in order to produce physically viable solutions is 2π, as detailed in Appendix B. Since k is dependent on β and, in turn, on α, we find its maximum value corresponding to $k = 2\pi$. The inverse proportionality of surface separation d and surface charge density σ (see equation (14)) restricts solutions to an interval where both d and σ cannot change arbitrarily, but are imposing an upper limit on one another by the equation

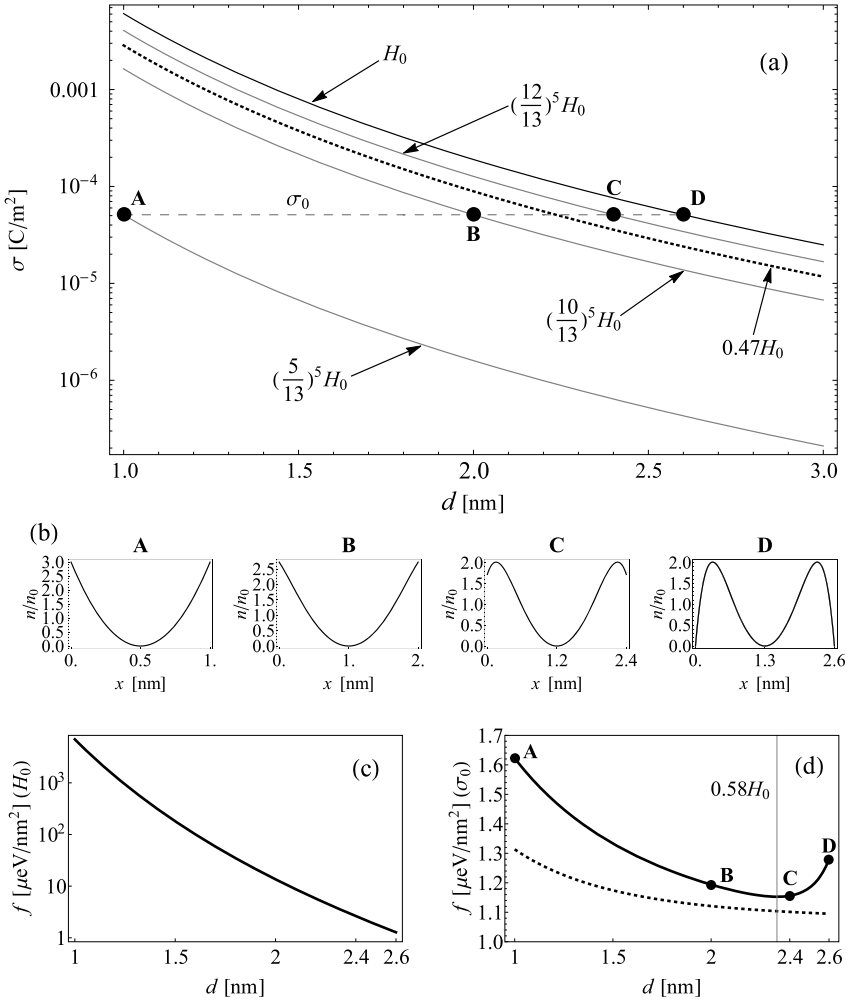

Fig. 2. Phase space of solutions, corresponding particle distributions $n(x)$ and Helmholtz free energy; (a): A portion of the phase space (d, σ) of particle distribution solutions (equation (27)). Arrows indicate isohypses of constant product σd^5, along which k is constant. From **A** to **D**, particle density changes continuously. At point **A**, $k = 1.05$. At point **D**, $k = 2\pi$. The isohypse $0.47H_0$ marks the transition of particle concentration being largest at the surfaces; (b): Particle density distributions $n(x)$ (equation (25)) for points **A**–**D** of the phase space in Fig. 2(a). The surface charge density is kept constant $\sigma_0 = 51\mu\text{C/m}^2$ while distance d between the surfaces increases from 1 nm to 2.6 nm; (c): Helmholtz free energy (equation (28)) along isohypses is a monotonous, power law dependent function of both d and σ. Here, the energy dependence along the isohypse H_0 is shown; (d): Full line: Helmholtz free energy along constant surface charge $\sigma_0 = 51\mu\text{C/m}^2$ (Fig. 2(a)). The points **A**–**D** correspond to points of the phase space of Fig. 2(a). Dashed line: Helmholtz free energy at identical parameters for original solutions ([36]). Free energy has a local minimum at $0.58H_0$.

$$\sigma d^5 = \left(\frac{h^2\varepsilon_0}{me_0^{5/3}}\right)^3 \left(\frac{3^6 \cdot 5^4 \cdot \pi^2}{2^{13}}\right)^{1/3} \equiv H_0, \tag{27}$$

where it is convenient to mark the many constants by H_0. At chosen surface separation d, the value of surface charge density can therefore at most be $\sigma = H_0/d^5$. The phase space (d, σ) consists of inversely proportional quintic curves, or isohypses (Fig. 2(a)). A short calculation confirms that at constant product σd^5 the parameter k is also constant, which in turn results in identical electric potential and number density dependencies. In a geometrical sense we find that moving along isohypses of constant product σd^5 results in identical $\phi(x)$ and $n(x)$, but not total Helmholtz free energy, as we shall soon see. The particle distributions $n(x)$ for four points of the phase space in Fig. 2(a) are shown in Fig. 2(b).

Calculations were performed with Wolfram Mathematica software (Wolfram Research, Inc., Mathematica, Version 9.0, Champaign, IL (2012)). The solutions for electric potential coincide with those found in [36]; electric potential is highest in the vicinity of the charged plates, where the electrons accumulate due to electrostatic attraction, and then decreases towards the middle of the surfaces, where the electric field is zero. The Pauli exclusion principle prevents the electrons to entirely condensate on both surfaces, so they are forced into higher-state energies or further away from the charged surfaces. This can be seen in Fig. 2(b), where the number density assumes a parabolic shape with zero concentration in the middle. At unchanging but arbitrary d and the limit $\sigma \to 0$ the particle distributions limit toward Fig. 2(b, **A**). This is in contrast with solutions discussed in [36], where in the limit of small σ the particles tend to distribute equidistantly between the surfaces. This non-uniform distribution hints at higher baseline equilibrium energies of the new solutions, as greater particle density implies occupation of higher energy states.

We find that particle density distributions start to change as soon as the product σd^5, or rather k, increases. It is perhaps most intuitive to fix one of the values, either d or σ, and investigate how electric potential or particle density change in dependence on only the other parameter. We may vary d from 1 nm to 2.6 nm at constant σ_0 and observe the change in $n(x)$, as shown in Fig. 2(b). In the initial parabolic distribution, most particles are accumulated near the surfaces. We find that the changes in $n(x)$ are continuous as the surfaces are brought apart. At a point beyond $0.47H_0$ on the phase space, the initial parabolic distribution with most particles accumulated near the surfaces gradually changes (Fig. 3); particles are steadily depleted from the immediate vicinity of the charged surfaces (Fig. 2(b, **C**)) until the concentration directly near the sur-

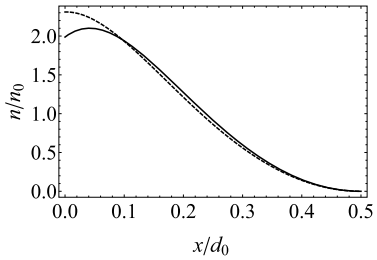

Fig. 3. Particle density distributions for isohypses $0.47H_0$ (dashed line, $d_0 = 2.24$ nm) and $0.58H_0$ (full line, $d_0 = 2.34$ nm). The surface charge density in both cases is $\sigma_0 = 51\,\mu\mathrm{C/m}^2$. The distribution is shown only for one half of the system due to symmetry.

faces drops to zero at H_0. Remarkably, fermion concentration in this regime is negligible near the surfaces but attains two localized peaks before decreasing to zero in the middle (Fig. 2(b, **D**)). It is possible that this energetically most favorable state corresponds to a metastable solution with electron wave-functions acting as bridging mediators between the surfaces. Reminiscing a standing wave function probability density of an infinite potential well with a boundary condition of electric field symmetry, one could argue that the fermions' wave functions are in phase, overlapping in a way that produces two localized peaks of number density in the limit of $k = 2\pi$. Further work could investigate the density of states with the Wentzel–Kramers–Brillouin (WKB) approximation, but this exceeds the scope of the present paper.

Helmholtz free energy per unit area (or simply, free energy) of the system at given values of d and σ is evaluated as the integral

$$f(d,\sigma) = f_0 \int_0^1 \left(\alpha n^{5/3}(x) + E^2(x)\right) \mathrm{d}x. \tag{28}$$

Here, the first term corresponds to energy density due to Fermi–Dirac wave function symmetry constraints of fermions (F_{sym}), while the second term is the energy of the mean electric field (F_{el}) (see equation (8)). Free energy is normalized with f_0, the surface energy density of a classical plate capacitor in a vacuum given by $f_0 = \sigma^2 d/2\varepsilon_0$. We are interested in seeing how free energy changes with d or σ. The two obvious approaches to achieving this are again along isohypses or parallel to one of the axes. Free energy along isohypses changes significantly. Fig. 2(c) shows the total free energy along the isohypse H_0. We see that the change in d spanning from one to two nanometers corresponds to around 2 orders of magnitude decrease in free energy, since the latter is a non-linear function of electric field, and in turn, of σ. This exponential dependence is a direct consequence of the power law present in equation (27) and the fact that both contributions to free energy are non-linear in nature, particularly F_{sym} (see [36]). This property could be useful in energy storage devices, as the slightest change in surface charge or surface separation would considerably change the energy of the system. A similar effect for small vacuum gaps has been reported on in recent literature [33]. In [36], we have kept surface charge constant while increasing surface separation and observed a similar trend of inversely proportional free energy dependence, but this is not the case with new solutions. Remarkably, free energy has a local minimum on the phase space when d and σ are in such proportions that

$$\sigma d^5 \approx 0.58 H_0. \tag{29}$$

This energy minimum is always greater in relation to the original solution at identical parameters. An example of this is shown in Fig. 2(d). We fix the surface charge to $\sigma_0 = 51\,\mu\mathrm{C/m}^2$ and vary the distance d from 1 to 2.6 nm. At first, the energy is decreasing until it reaches a local minimum at approximately $d = 2.34$ nm before increasing again. This result is surprising as our previous calculations always predicted the free energy to be a monotonous, and decreasing, function of surface separation (see Fig. 2(d)). Distance-dependent free energy decrease is intuitive, not only because electric fields are weaker at greater distances, but because F_{sym} significantly levels off with more space available to the fermions ([36]). When equation (29) is fulfilled, the net force between the surfaces is zero, yet becomes attractive when the free energy gradient is positive, from $0.58H_0$ to H_0. For $d = 1$ nm, the attractive force is of order of piconewtons per square nanometer. Fig. 2(d) illustrates that the free energy of the primary solution ([36]) is always lower for identical parameters. It is possible that this points to a metastable character of the new solutions, corresponding to new and volatile physical states that were lost when taking only the positive root of equation (15). It is tempting to think of the attraction as being Casimir-like in origin, as there is no assumptions of a physical medium: the vacuum between the surfaces is permeated only by electric field $E(x)$ and wave functions of electrons. However, it is rather difficult to continue this argument within the confines of the present model.

Most elusive to interpretation is perhaps the non-monotonous number density distribution $n(x)$ seen in Fig. 2(b). In the case of primary solutions, particle density is greatest at the charged surfaces and levels off towards the middle, with the overall attraction being repulsive. Contradictory to this, new solutions result in particle concentration that does not seem to be greatest directly at the surfaces, but somewhat farther away. Since all our solutions correspond to thermodynamic equilibrium minima of free energy, it is possible that such configurations are most effective at shielding the electric field of the surfaces, overall minimizing the mean electric field energy throughout the pore. Consequently, the wave functions of the electrons overlap in ways that result in highest concentration of states somewhere between the charged surface and the mid-line. Beyond $0.58H_0$, particles are concentrated in two peaks (see Fig. 2(b), **C**–**D**), effectively shielding the repulsion of the plates. The surfaces are attracted to these two areas of converged opposite charge, resulting in an overall attraction of the two surfaces.

As discussed in the introduction, attraction between like-charged surfaces is not uncommon in nature. On a molecular scale, it is known that like-charged surfaces are commonly attracted to each other in the presence of multivalent counterions and spherical particles with a quadrupolar charge distribution [39,42–45]. A common mechanism of the latter is the so-called bridging mediation. Quadrupolar particles have a charge at opposite sides of the diameter, where one of the sides is adsorbed to the differently charged surface. If the gap between charged surfaces is a factor of the particle's diameter, orientational ordering arranges the particles into chains that bridge the gap of both surfaces, consequently pulling them together. Such a result cannot be predicted by the classic Poisson–Boltzmann theory, which is a first-order approximation for weak electric fields and low particle concentrations. Attraction between like-charged surfaces has been reported in Monte-Carlo simulations of electrolytes for high counterion-surface coupling parameters [40,50]. Similar theoretical results were reported for high counterion valencies, high surface charge densities and low temperatures [49].

Although our model rests on assumptions that are wholly of a quantum mechanical origin, we may draw some parallels with these findings. Quantum mechanical formulation implies implicit correlation between fermions; the particles are not independent, but rather strongly correlated by the Pauli exclusion principle. We have seen that attraction between the surfaces happens only in the vicinity of relatively high surface charge σ, moreover when

particles are depleted from the surfaces, being relocated roughly half-way towards the middle. This concentration of charge creates an attractive force between each surface and particle cluster, reminiscent of a system of two plane parallel capacitors in series. It would be interesting to investigate how this attraction would change if our model included electric field influence on the wave functions. Although particles are point-like, these perturbed states would possess a certain anisotropy, possibly resulting in a sort of orientational ordering and further amplifying the bridging attraction effect. Furthermore, an inclusion of a Coulomb interaction term would also be appropriate now that the effects of Fermi–Dirac statistics were singled out. We predict that this addition would alter the resulting particle distributions at higher densities – at the cost of possibly screening the subtler Fermi–Dirac interactions, rendering them unnoticeable.

The use of density functional theory for a semiclassical description of many-electron systems is not new, having been introduced by the Thomas–Fermi model in the study of ground state atoms. It differs from a density wavefunction approach by instead considering the number density of electrons, finding the spherical momentum space up to Fermi momentum. The shortcomings of this theory were addressed by the Kohn–Sham density functional theory and others ([51], [52]). Later, the formalism based on the density has been generalized to other systems consisting of many particles, in particular, constituents of ionic solutions [53]. Due to the large particle numbers the methods of statistical physics are appropriate. In considering the electric double layer, the functional depends on the global system – charged surfaces and electrons between them – so the functions are expected to vary with the distance between the surfaces. On the other hand, the use of ensamble statistics requires the fields to be constant within the representative subsystem. It is therefore necessary to first consider local thermodynamic equilibrium by dividing the system into infinitesimal slices and assuming equilibrium of each slice. Here, the electrons can be considered as explicitly independent and are described as dimensionless particles by the Schrödinger equation [37]. The density functional is in our model introduced when parts of the system are assembled into a global system with spatially varying electric field and density of the number of fermions, similarly to the model of electrolyte solution [26].

4. Conclusions

We have presented new solutions to our model of a capacitor with quantum particles that are restricted by Fermi–Dirac statistics. Constructing a free energy functional and using calculus of variations, we have derived an analytical approximation for the number density of particles, electric potential within the capacitor and free energy. The phase space of solutions are isohypses of a constant product of two model parameters. We have found that free energy changes by a power law along isohypses, but has a local minimum when one of the parameters is held constant. Remarkably, this implies an attraction between two like-charged surfaces, a result that is analogous to attraction of like-charged surfaces on a molecular scale and ubiquitous in natural processes. Potential applications of our research are in energy storage technologies, particularly in nano gap capacitors and vacuum microcathode arrays. With engineering increasingly moving into the nano scales, research in possible quantum effects is necessary. Upgrades to our model would consider the effects of electric fields on wave functions and dissipation processes, such as leakage currents.

Acknowledgements

This work was supported by the Slovenian Research Agency (ARRS) grants P3-0388, J1-6728 and J5-7098.

Appendix A. Derivation of electric potential

We start by considering equation (21). Since $(-1)^{3/2} = i$, where i is the imaginary unit,

$$\frac{\mathrm{d}^2\phi}{\mathrm{d}x^2} = (-i)\left(\frac{\beta\sqrt{5}}{4}\right)^3 (\tilde{\lambda} - 4\phi)^{3/2}. \tag{A.1}$$

We introduce a new variable

$$u = \tilde{\lambda} - 4\phi, \qquad \mathrm{d}u = -4\,\mathrm{d}\phi, \tag{A.2}$$

and make use of the identity

$$\frac{\mathrm{d}}{\mathrm{d}x}\left(\frac{\mathrm{d}\phi}{\mathrm{d}x}\right)^2 = 2\frac{\mathrm{d}\phi}{\mathrm{d}x}\frac{\mathrm{d}^2\phi}{\mathrm{d}x^2}. \tag{A.3}$$

Multiplying both sides of equation (A.1) by $2\,\mathrm{d}\phi/\mathrm{d}x$,

$$2\frac{\mathrm{d}\phi}{\mathrm{d}x}\frac{\mathrm{d}^2\phi}{\mathrm{d}x^2} = 2\frac{\mathrm{d}\phi}{\mathrm{d}x}(-i)\Big[\frac{5\sqrt{5}\beta^3}{64}\Big]u^{3/2} \tag{A.4}$$

and using the chain rule

$$\frac{\mathrm{d}u}{\mathrm{d}x} = \frac{\mathrm{d}u}{\mathrm{d}\phi}\frac{\mathrm{d}\phi}{\mathrm{d}x}, \tag{A.5}$$

we can rewrite equation (A.4):

$$\frac{\mathrm{d}}{\mathrm{d}x}\left(\frac{\mathrm{d}u}{\mathrm{d}x}\cdot\frac{\mathrm{d}\phi}{\mathrm{d}u}\right)^2 = 2\left(\frac{\mathrm{d}u}{\mathrm{d}x}\cdot\frac{\mathrm{d}\phi}{\mathrm{d}u}\right)(-i)\Big[\frac{5\sqrt{5}\beta^3}{64}\Big]u^{3/2}. \tag{A.6}$$

Since $\mathrm{d}\phi/\mathrm{d}u = -1/4$, it follows that

$$\frac{1}{16}\mathrm{d}\left(\frac{\mathrm{d}u}{\mathrm{d}x}\right)^2 = \frac{i}{2}\Big[\frac{5\sqrt{5}\beta^3}{64}\Big]u^{3/2}\mathrm{d}u. \tag{A.7}$$

We integrate both sides of equation (A.7) from $x = 1/2$, where the reduced potential value is $u_{1/2}$ and electric field strength $\mathrm{d}u/\mathrm{d}x$ is zero due to symmetry:

$$\left(\frac{\mathrm{d}u}{\mathrm{d}x}\right)^2 = \Big[\frac{\sqrt{5}\beta^3}{4}\Big]i(u^{5/2} - u_{1/2}^{5/2}). \tag{A.8}$$

Before taking the root and integrating again, we approximate the power 5/2 on the right hand side by 2 to keep the integral analytical. As discussed in [36], the deviation of this approximation is numerically negligible. The integral limits run from $x = 1/2$ to some arbitrary $1/2 < x < 1$, with the corresponding reduced potential limits running from $u_{1/2}$ to $u(x)$:

$$\frac{u + \sqrt{u^2 - u_{1/2}^2}}{u_{1/2}} = \exp\left(c(\frac{1}{2} - x)\right). \tag{A.9}$$

Here, $c = (1+i)5^{1/4}\beta^{3/2}/2\sqrt{2}$, where $(1+i)$ comes from the square root of the imaginary unit $\sqrt{i} = (\sqrt{2}/2)(1+i)$. After some rearranging we derive the expression for the reduced potential $u(x)$:

$$u = u_{1/2}\cosh\left(c(x - \frac{1}{2})\right). \tag{A.10}$$

Considering the identity for complex arguments of hyperbolic functions

$$\cosh(a + bi) = \cosh a\cos b + i\sinh a\sin b, \tag{A.11}$$

we may separate the reduced potential dependency into a sum of real and complex terms, namely

$$u = u_{1/2}\Big(\cosh k(x-\frac{1}{2})\cos k(x-\frac{1}{2}) + i\sinh k(x-\frac{1}{2})\sin k(x-\frac{1}{2})\Big), \tag{A.12}$$

where the constant k is now real and equal to

$$k = \frac{5^{1/4}}{2}\sqrt{\frac{\beta^3}{2}}. \tag{A.13}$$

The constant $u_{1/2}$ is determined from the boundary condition of electric field $\mathrm{d}\phi(x=0)/\mathrm{d}x = -1$ (equation (19)). Accounting for substitution u (equation (A.2)) and taking only the real component of potential, we get

$$\Re(\frac{\mathrm{d}u}{\mathrm{d}x})\Big|_{x=0} = -4\frac{\mathrm{d}\phi}{\mathrm{d}x}\Big|_{x=0} = (-4)\cdot(-1) = 4. \tag{A.14}$$

Here, $\Re(z)$ denotes the real part of imaginary number z. The derivative $\mathrm{d}u/\mathrm{d}x$ is equal to

$$\frac{\mathrm{d}u}{\mathrm{d}x} = (1+i)ku_{1/2}\sinh\Big(k(1+i)(x-\frac{1}{2})\Big), \tag{A.15}$$

its real part being

$$\Re(\frac{\mathrm{d}u}{\mathrm{d}x}) = ku_{1/2}\Big(\cos k(x-\frac{1}{2})\sinh k(x-\frac{1}{2}) - \cosh k(x-\frac{1}{2})\sin k(x-\frac{1}{2})\Big). \tag{A.16}$$

Considering equation (A.14), we find $u_{1/2}$:

$$u_{1/2} = \frac{4}{k\left(\cosh\frac{k}{2}\sin\frac{k}{2} - \cos\frac{k}{2}\sinh\frac{k}{2}\right)}. \tag{A.17}$$

We can finally write the real component of the reduced potential $u(x)$:

$$\Re(u(x)) = \frac{4\cos\left(k(x-\frac{1}{2})\right)\cosh\left(k(x-\frac{1}{2})\right)}{k\left(\cosh\frac{k}{2}\sin\frac{k}{2} - \cos\frac{k}{2}\sinh\frac{k}{2}\right)}. \tag{A.18}$$

What is left is determining the Lagrange multiplier $\tilde{\lambda}$. We find it by considering equation (A.2) and the zero of potential $\phi(x)$ (equation (18)):

$$\phi(x=\frac{1}{2}) = \frac{\tilde{\lambda} - \Re(u(x=\frac{1}{2}))}{4} = 0 \quad\longrightarrow\quad \tilde{\lambda} = \frac{4}{k\left(\cosh\frac{k}{2}\sin\frac{k}{2} - \cos\frac{k}{2}\sinh\frac{k}{2}\right)}. \tag{A.19}$$

By using equations (A.2) and (A.18) we obtain the dependence of the potential ϕ on coordinate x (equation (22)):

$$\phi(x) = \frac{1-\cos\left(k(x-\frac{1}{2})\right)\cosh\left(k(x-\frac{1}{2})\right)}{k\left(\cosh\frac{k}{2}\sin\frac{k}{2} - \cos\frac{k}{2}\sinh\frac{k}{2}\right)}. \tag{A.20}$$

Appendix B. Analysis of $n(x) \geq 0$ condition

When analyzing the condition for $n(x) \geq 0$, we are interested in zeros of the numerator of equation (25):

$$k\sin k(x-\frac{1}{2})\sinh k(x-\frac{1}{2}) \geq 0. \tag{B.1}$$

Since k is defined by positive constants, the trivial solution $k=0$ is not possible. The normalization of the coordinate x in equation (11) assures the domain is $x \in [0,1]$. When $x > 1/2$, the whole expression will be positive, and likewise for $x < 1/2$, since both sine and hyperbolic sine are odd functions. Next, particle density at $x = 1/2$ will always be zero. Non-trivial solutions require $\sin k(x-1/2)$ to be zero, imposing the condition

$$\sin k(x-\frac{1}{2}) = 0 \quad\longrightarrow\quad k = \frac{q\pi}{(x-1/2)}, \quad q = 1,2,3\ldots, \tag{B.2}$$

where q is an integer since k is defined by positive constants. Plotting $n(x)$ on the interval $[0,1]$ we find that k can indeed vary from 0 to 2π with the function being non-negative on the domain. Further products of 2π render particle density negative, as seen in Fig. B.4. It is therefore conclusive that the maximum value of k is 2π.

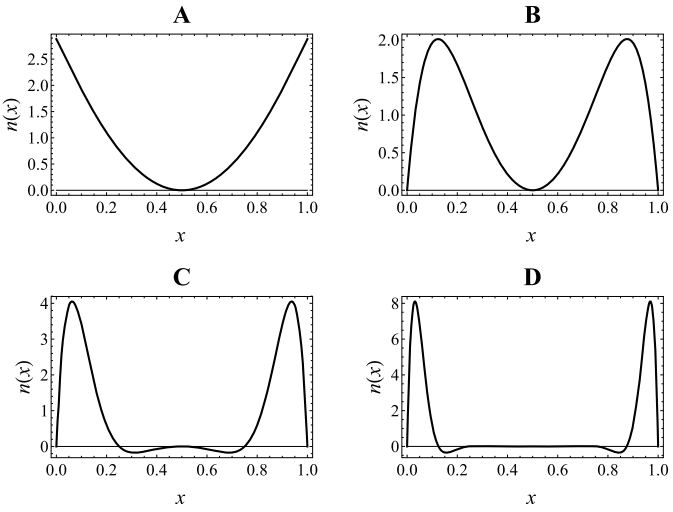

Fig. B.4. Particle density functions (equation (25)) for different values of k. (A): $k=\pi$; (B): $k=2\pi$; (C): $k=4\pi$; (D): $k=8\pi$.

References

[1] A. Miodek, G. Castillo, T. Hianik, H. Korri-Youssoufi, Electrochemical aptasensor of human cellular prion based on multiwalled carbon nanotubes modified with dendrimers: a platform for connecting redox markers and aptamers, Anal. Chem. 85 (2013) 7704–7712.
[2] P. Kowalczyk, A. Ciach, A.P. Terzyk, P.A. Gauden, S. Furmaniak, Effects of critical fluctuations on adsorption-induced deformation of microporous carbons, J. Phys. Chem. C 119 (2015) 6111–6120.
[3] R. Imani, M. Pazoki, A. Tiwari, G. Boschloo, A.P.F. Turner, V. Kralj-Iglič, et al., Band edge engineering of TiO2@DNA nanohybrids and implications for capacitive energy storage devices, Nanoscale 7 (2015) 10438–10448.
[4] M. Kulkarni, Y. Patil-Sen, I. Junkar, C.V. Kulkarni, M. Lorenzetti, A. Iglič, Wettability studies of topologically distinct titanium surfaces, Colloids Surf. B 129 (2015) 47–53.
[5] R. Imani, M. Pazoki, D. Zupanč ič, M.E. Kreft, V. Kralj-Iglič, P. Veranič, et al., Biocompatibility of different nanostructured TiO2 scaffolds and their potential for urologic applications, Protoplasma 253 (2015) 1439–1447.
[6] R. Imani, R. Dillert, D.W. Bahnemann, M. Pazoki, T. Apih, V. Kononenko, et al., Multifunctional gadolinium-doped mesoporous TiO2 nanobeads: photoluminescence, enhanced spin relaxation, and reactive oxygen species photogeneration, beneficial for cancer diagnosis and treatment, Small 13 (2017) 1700349.
[7] J.A. Manzanares, S. Mafé, J. Bisquert, Electric double layer at the membrane/solution interface: distribution of electric potential and estimation of the charge stored, Ber. Bunsenges. 96 (1992) 538–544.
[8] I. Bivas, Electrostatic and mechanical properties of a flat lipid bilayer containing ionic lipids colloids, Colloids Surf. A 282–283 (2006) 423–434.
[9] M. Kulkarni, A. Mazare, J. Park, E. Gongadze, M.S. Killian, S. Kralj, et al., Protein interactions with layers of TiO2 nanotube and nanopore arrays: morphology and surface charge influence, Acta Biomater. 45 (2016) 357–366.
[10] X. Chen, Z. Guo, G.M. Yang, J. Li, M.Q. Li, J.H. Liu, et al., Electrical nanogap devices for biosensing, Mater. Today 13 (2010) 28–41.

[11] R.D. Munje, S. Muthukumar, A.P. Selvam, S. Prasad, Flexible nanoporous tunable electrical double layer biosensors for sweat diagnostics, Sci. Rep. 5 (2015) 14586.
[12] K. Kaliyappan, Z. Chen, Atomic-scale manipulation of electrode surface to construct extremely stable high-performance sodium ion capacitor, Nano Energy 48 (2018) 107–116.
[13] S.L. Candelaria, Y. Shao, W. Zhou, X. Li, J. Xiao, J.G. Zhang, et al., Nanostructured carbon for energy storage and conversion, Nano Energy 1 (2012) 195–220.
[14] Y. Chen, F. Trier, T. Kasama, D.V. Christensen, N. Bovet, Z.I. Balogh, et al., Creation of high mobility two-dimensional electron gases via strain induced polarization at an otherwise nonpolar complex oxide interface, Nano Lett. 15 (2015) 1849–1854.
[15] R. Costa, C.M. Pereira, A.F. Silva, Insight on the effect of surface modification by carbon materials on the ionic liquid electric double layer charge storage properties, Electrochim. Acta 176 (2015) 880–886.
[16] R. Signorelli, D.C. Ku, J.G. Kassakian, J.E. Schindall, Electrochemical double-layer capacitors using carbon nanotube electrode structures, Proc. IEEE 97 (2009) 1837–1847.
[17] H. Du, H. Yang, C. Huang, J. He, H. Liu, Y. Li, Graphdiyne applied for lithium-ion capacitors displaying high power and energy densities, Nano Energy 22 (2016) 615–622.
[18] S. McLaughlin, The electrostatic properties of membranes, Annu. Rev. Biophys. Biophys. Chem. 18 (1989) 113–136.
[19] M.G. Gouy, Sur la constitution de la charge électrique à la surface d'un électrolyte, J. Phys. (Paris) 9 (1910) 457–468.
[20] D.L. Chapman, A contribution to the theory of electrocapillarity, Philos. Mag. 6 (1913) 475–481.
[21] R. Parsons, The electrical double layer: recent experimental and theoretical developments, Chem. Rev. 90 (1990) 813–826.
[22] O. Stern, Zur Theorie der elektrolytischen Doppeltschicht, Z. Elektrochem. 30 (1924) 508–516.
[23] M. Eigen, E. Wicke, The thermodynamics of electrolytes at higher concentration, J. Phys. Chem. 58 (9) (1954) 702–714.
[24] V. Freise, Zur theorie der diffusen doppelschicht, Z. Elektrochem. Ber. Bunsenges. Phys. Chem. 56 (8) (1952) 822–827.
[25] I. Borukhov, D. Andelman, H. Orland, Steric effects in electrolytes: a modified Poisson–Boltzmann equation, Phys. Rev. Lett. 79 (1997) 435.
[26] V. Kralj-Iglič, A. Iglič, A simple statistical mechanical approach to the free energy of the electric double layer including the excluded volume effect, J. Phys. II 6 (1996) 477–491.
[27] J.J. Bikerman XXXIX, Structure and capacity of electrical double layer, Lond. Edinb. Dubl. Philos. Mag. J. Sci. 33 (1942) 384–397.
[28] C. Merlet, D.T. Limmer, M. Salanne, R. Van Roij, P.A. Madden, D. Chandler, B. Rotenberg, The electric double layer has a life of its own, J. Phys. Chem. C 118 (32) (2014) 18291–18298.
[29] A. Velikonja, V. Kralj-Iglič, A. Iglič, On asymmetric shape of electric double layer capacitance curve, Int. J. Electrochem. Sci. 10 (2015) 1–7.
[30] E. Gongadze, U. van Rienen, V. Kralj-Iglič, A. Iglič, Langevin Poisson–Boltzmann equation: point-like ions and water dipoles near a charged surface, Gen. Physiol. Biophys. 30 (2011) 130–137.
[31] E. Gongadze, A. Iglič, Asymmetric size of ions and orientational ordering of water dipoles in electric double layer model – an analytical mean-field approach, Electrochim. Acta 178 (2015) 541–545.
[32] C. Ionescu-Zanetti, J.T. Nevill, D.D. Carlo, K.H. Jeong, L.P. Lee, Nanogap capacitors: sensitivity to sample permittivity changes, J. Appl. Phys. 99 (2) (2006) 1.
[33] D. Lyon, A. Hubler, Gap size dependence of the dielectric strength in nano vacuum gaps, IEEE Trans. Dielectr. Electr. Insul. 20 (4) (2013) 1467–1471.
[34] N.D. Lang, W. Kohn, Theory of metal surfaces: charge density and surface energy, Phys. Rev. B 1 (1970) 4555–4568.
[35] A. Hubler, S. Foreman, J. Liu, L. Wortsmann, Large energy density in three-plate nanocapacitors due to Coulomb blockade, J. Appl. Phys. 123 (10) (2018) 103302.
[36] M. Drab, V. Kralj-Iglič, Diffuse electric double layer in planar nanostructures due to Fermi–Dirac statistics, Electrochim. Acta 204 (2016) 154–159.
[37] T.L. Hill, An Introduction to Statistical Thermodynamics, third ed., Dover Publications Inc., New York, 1986.
[38] R. Kjellander, S. Marč elja, R.M. Pashley, J.P. Quirk, Double-layer ion correlation forces restrict calcium-clay swelling, J. Phys. Chem. 92 (1988) 6489.
[39] J. Urbanija, K. Bohinc, A. Bellen, S. Maset, A. Iglič, V. Kralj-Iglič, P.S. Kumar, Attraction between negatively charged surfaces mediated by spherical counterions with quadrupolar charge distribution, J. Chem. Phys. 129 (2008) 105101.
[40] J. Zelko, A. Iglič, V. Kralj-Iglič, P.S. Kumar, Effects of counterion size on the attraction between similarly charged surfaces, J. Chem. Phys. 133 (2010) 204901.
[41] K. Bohinc, J. Zelko, P.S. Kumar, A. Iglič, V. Kralj-Iglič, Attraction of like-charged surfaces mediated by spheroidal nanoparticles with spatially distributed electric charge: theory and simulation, Adv. Planar Lipid Bilayers Liposomes 9 (2009) 279–301.
[42] Y. Levin, Electrostatic correlations: from plasma to biology, Rep. Prog. Phys. 65 (2002) 1577.
[43] N. Ise, T. Konishi, B.V.R. Tata, How homogeneous are "homogeneous dispersions"? Counterion-mediated attraction between like-charged species, Langmuir 15 (12) (1999) 4176–4184.
[44] K. Besteman, M.A. Zevenbergen, H.A. Heering, S.G. Lemay, Direct observation of charge inversion by multivalent ions as a universal electrostatic phenomenon, Phys. Rev. Lett. 93 (2004) 170802.
[45] S. May, K. Bohinc, Attraction between like charged surfaces mediated by uniformly charged spherical colloids in a salt solution, Croat. Chem. Acta 84 (2011) 251–257.
[46] K.M. Salerno, A.L. Frischknecht, M.J. Stevens, Charged nanoparticle attraction in multivalent salt solution: a classical-fluids density functional theory and molecular dynamics study, J. Phys. Chem. B 120 (2016) 5927–5937.
[47] R.H. French, V.A. Parsegian, R. Podgornik, R.F. Rajter, A. Jagota, J. Luo, et al., Long range interactions in nanoscale science, Rev. Mod. Phys. 82 (2) (2010) 1887.
[48] X. Zhang, J.S. Zhang, Y.Z. Shi, X.L. Zhu, Z.J. Tan, Potential of mean force between like-charged nanoparticles: many-body effect, Sci. Rep. 6 (2016) 23434.
[49] A.G. Moreira, R.R. Netz, Binding of similarly charged plates with counterions only, Phys. Rev. Lett. 87 (7) (2001) 078301.
[50] A.P. dos Santos, R.R. Netz, Dielectric boundary effects on the interaction between planar charged surfaces with counterions only, J. Chem. Phys. 148 (16) (2018) 164103.
[51] P. Hohenberg, W. Kohn, Inhomogeneous electron gas, Phys. Rev. 136 (3B) (1964) B864.
[52] W. Kohn, L.J. Sham, Self-consistent equations including exchange and correlation effects, Phys. Rev. 140 (4A) (1965) A1133.
[53] D.W. Gruen, S. Marčelja, Spatially varying polarization in water. A model for the electric double layer and the hydration force, J. Chem. Soc. Faraday Trans. II 79 (2) (1983) 225–242.
[54] D.T. Thoai, E. Zeitler, Image potential of an electron in a gap between two metals, Phys. Status Solidi (b) 146 (1) (1988) 137–140.